The design of specific flat mechanical test specimen and grips for use in a cryogenic self-reacting environmental chamber

Parthasarathy Iyengar, Materials & Processes Engineer - Airbus;
Dr. Shwe Soe, Associate Professor - University of West of England

Date 03rd October 2023

Airbus AMBER

Contents

Airbus AMBER

References

1) Thomas, M, Flynn, “Cryogenic Engineering”, 2nd Edition, 2005, Taylor & Francis Group LLC, ISBN 13: 978-0-8247-5367-2 (hbk)

2) Walter D. Pilkey, Deborah F. Pilkey, “Peterson’s Stress Concentration Factors”, 3rd Edition, 2008, John Wiley & Sons Inc. ISBN 978-0-470-04824-5 (cloth)

3) MMPDS- 14 , [Washington, D.C.] : Federal Aviation Administration ; [Columbus, Ohio] : Battelle Memorial Institute, [2019]

4) EFFECT OF HEAT TREATMENT ON THE MECHANICAL PROPERTIES OF ALUMINUM ALLOY 2219 AND ITS WELDED JOINTS AT CRYOGENIC AND ELEVATED TEMPERATURES; E. V. Vorobyov and others; Strength of Materials, Vol. 54, No. 2, March, 2022; DOI 10.1007/s11223-022-00402-6

5) EN 6072:2010 - Aerospace series - Metallic materials - Test methods - Constant amplitude fatigue testing; CEN approved on 25 December 2009; ICS 49.025.05

6) Ramberg, W., & Osgood, W. R. (1943). Description of stress–strain curves by three parameters. Technical Note No. 902, National Advisory Committee For Aeronautics, Washington DC.

7) Xiuru Li; Effect of cryogenic temperatures on the mechanical behaviour and deformation mechanism of AISI 316H stainless steel; Dalian University of Technology, 116024, PRC

8) “Zum Einflub der Nietnachgiebigkeit mehrreihiger Nietverbindungen auf die Lastübertragungs- und Lebensdauervorhersage,” LBF Report No. FB-172, dissertation, Technische Universität München, Munich, Germany, 1984

9) McCarthy CT and Gray PJ. An analytical model for the prediction of load distribution in highly torqued multi-bolt composite joints. Composite Structures 2011; 92(2): 287-298.

10) M. JAVADI , M. TAJDARI; Experimental investigation of the friction coefficient between aluminium and steel; Materials Science-Poland, Vol. 24, No. 2/1, 2006; Islamic Azad Univ., Iran

11) Fastener Design Manual, Richard T. Barrett, NASA_RP-1228, March 1990.

12) ASD-STAN prEN 6115:2019; Aerospace series — Bolt — Protruding head, Short thread — Inch series; ASD-STAN, Rue Montoyer, 10/5 - B-1000 Brussels, Belgium

1. Background and objective

Background – reason for motivation

- Airbus announced the ambition to design more environmentally friendly aircraft as part of the ZEROe initiative in Q3, 2020.
- Four hydrogen powered aircraft concepts were unveiled.

Turbofan
Range: 2,000+ nm | Passengers: <200

Turboprop
Range: 1,000+ nm | Passengers: <100

Blended-Wing Body (BWB)
Range: 2,000+ nm | Passengers: <200

Fully electrical concept
Range: 1,000 nm | Passengers: <100

- Methods of propulsion involved both the use of hydrogen combustion and hydrogen fuel cells.
- In the case of hydrogen combustion, gas turbines with modified fuel injectors and fuel systems are powered with hydrogen in a similar manner to how aircraft are powered today. *Use of cryogenic hydrogen was a consideration.*
- A second method, hydrogen fuel cells, creates electrical energy which in turn powers electric motors that turn a propeller or fan. This is a fully electric propulsion system, quite different to the propulsion system on aircraft currently in service.
- When this was unveiled internally, the Materials and Processes team within the incumbent organisation structure pro-actively attempted to address challenges of materials characterization and associated testing. This work is a by-product.

Background – **Dry, Low Temperature test**

- Considering the current day practice of material testing at production batch level by suppliers in order to ensure quality, it was perceived that the same would apply to cryogenic hydrogen carrying materials.
- Material characterization and structural testing would have to be safely carried out considering both, the hazard of cryogens and the flammability of hydrogen.
- If low temperature behaviour could be isolated from the influence of hydrogen for characterization by the principle of superposition; safer solutions were seen to be plausible.
- To characterize the effect of cooling alone, a ‘dry’ mechanical test setup for fatigue – which could be employed using cryocooling and conveyor gas to replace cryogen (existing technology).
- A mechanical test setup was found most efficient by use of passive mechanical joint part, of a *self-reacting frame* instead of hydraulic grips.
- The specimen was selected to be a customization of the nett-section tested EN 6072 Open-hole “T-type” specimen. It is a fatigue test standard that is popularly employed by aerospace suppliers.

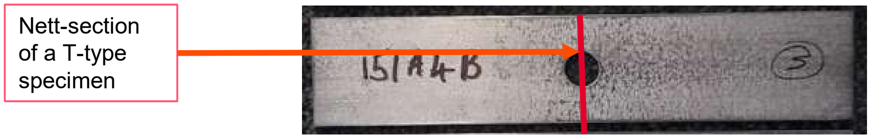

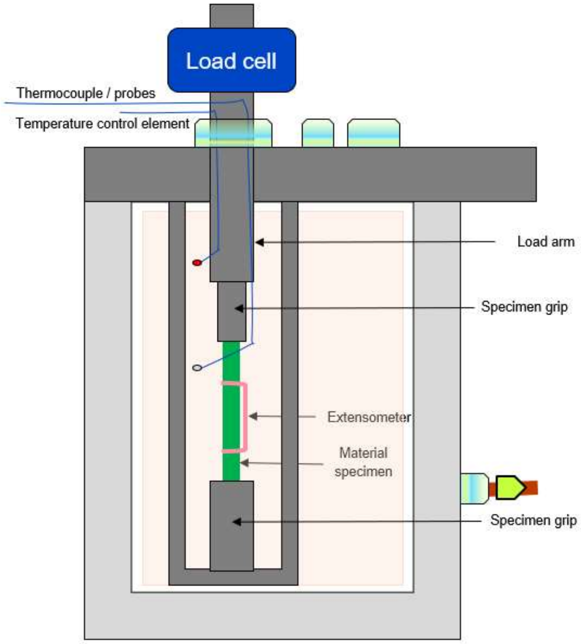

Objective

- The objective of this presentation is to discuss the design of modified T-type specimen and assembly as appropriate for use in a self-reacting environmental chamber.

- The specimen type is employed for determination of initiation by tensile fatigue and design is limited to applicability at R = 0.1.

- Aluminium 2024-T351 is selected as a basis for material of the specimen due to extensive availability of room temperature ("RT") material data [3], proximity to 2219-T6/T8 weldable alloys used in the space industry [4] and the ambition to use select Al. alloys for aircraft applications.

- Fatigue testing of modified 2024-T351 specimen employing the passive mechanical joint concept can be executed to compare with existing T-type coupon data at Room temperature.

- *Our objective is therefore to discuss design of a specifically modified coupon and assembly which may be used to demonstrate equivalence or provide a conservative 'read-across' to results produced by T-type coupon test at Room Temperature – so that the modified coupon may be applied to the characterization of cryogenic behaviour for aircraft application.*

- Finite Element Modelling using **Abaqus** is employed as a theoretical sizing and design tool for the scope and is not used to simulate measured behaviour from specific testing. Open source material data from MMPDS [3] is applied where practicable, for universal accessibility.

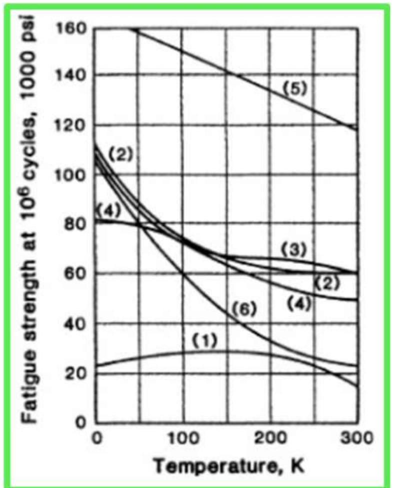

From [1]; (Y- axis is in ksi)
(1) 2024-T4
(2) Beryllium copper
(3) K. Monel
(4) Titanium
(5) 304 Stainless steel
(6) C1020 Carbon steel
(7) 9% Nickel
(8) Teflon

Note:
Fatigue strength is seen to increase with reduction in temperature.

2. Assumptions

Assumptions - general

- Static FEM uses non-linear stress-strain data approximated using an internal routine applying the Ramberg-Osgood approach [6] as basis to estimate the true stress. Strain at failure is taken to be those at UTS as indicated by exemplary curves in [3].
- Being ductile materials, the Von Mises stress criterion is used.
- Grip materials considered are metallic alone owing to convenient availability of definitive properties as open source data, on which we rely.
- Conventional loading clamps for Universal Testing are typically made of steel. In this case, AISI 316 is arbitrary assumed, given its high modulus (200 GPa) – despite lower strength at room temperature. Models account for this by a sufficiently high assigned thickness. As additional information, AISI 316 is understood to have much higher mechanical performance at low temperatures – hence may be a candidate to apply solely to cryogenic testing [7].
- Top-down mesh used for FEM and selection of surfaces instead of nodes for constraints result in small asymmetry, which are neglected given limitations of ‘machine acceptable’ linearity of loading, assembly asymmetry and material granularity. The models are taken to be reasonably representative.
- 4 bolt holes are arbitrarily assigned to the Grip and Lat Plates.
- 1-D bolts are modelled for sizing assuming global stiffness of 10E6 N/mm, much than specifically calculated Huth values [8] .
- Simplistic Abaqus damage modelling for estimation of fracture energy.
- Fatigue testing will operate in the ‘high cycle’ region i.e. maximum stress would correspond to 10,000 cycles. For 2024-T351, this is below 325 MPa [3].

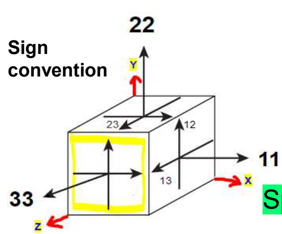

Specimen is loaded along z (’33’)

Design flow

Initially sized **cp1** Geometry → CAD / FEM study of assembly ⇄ Loops from Learning → Validation

Airbus AMBER

Assumptions - Materials considered [3]

	Material	Source	E MPa	G MPa	Calc G MPa	v	UTS MPa	TYS MPa	ρ g/cc	e %	ε % at UTS	Fsu MPa
1	Al 2024-T351 Plate (L)	AMS 4037 / MMPDS-14	73774 (10.7e3 Ksi)	25580 (4e3 Ksi)	27735 MPa	0.33	441 (A)	331 (A)	**2.76**	12	10	268 (A)
2	St AISI 316 Plate Sol. HT (L)	AMS 5524 MMPDS-14	**200000** (29e3 Ksi)	-	**80000** MPa	0.25*	503 (S)	179 (S)	7.91	40	9.5	344 (A)
3	St AISI 304 Sht (½ hard) (L)	AMS 5911 / MMPDS-14	179310 (26e3 Ksi)	72414 (10.5e3 Ksi)	70594 MPa	0.27	972 (A)	641 (A)	7.91	40	9.5	530 (A)
4	Al 2219-T851 Sheet/Plate (L)	AMS 4599 / MMPDS-14	72395 (10.5e3 Ksi)	25580 (4e3 Ksi)	27216 MPa	0.33	420 (A)	324 (A)	2.85	7	7	248 (A)
5	Ti-6Al-4v Bar Annealed (L)	AMS 4928 / MMPDS-14	116521 (16.9e3 Ksi)	42759 (6.2e3 Ksi)	44474 MPa	0.31	896 (A)	820 (A)	4.42	10	10	634 (S)
6	C465 H950 Steel bar (L/LT)	AMS 5936 MMPDS-14	**197880** (28.7e3 Ksi)	-	**77297** MPa	0.28	**1758** (A)	**1641** (A)	7.75	10	**10**	**923 (A)**

- **"Calc G" is G = E / 2*(1+v) - applied to FEM.**

Grip | Specimen | Clamp | Reference mat'l for grip/clamp

- Assumed properties are of the thinnest section just above the geometric requirement/assumption
- Thicker section properties are assumed for Ti-6Al-4v although thin sections are available

* assumed value from AK Steel (www.matweb.com)

Naming convention of assembly is based upon material as:

(coupon)(grip)(clamp)

ex. 432 – is (2219-T851)(AISI 304)(AISI 316)

3. Concept

Concept – about the EN 6072 T-type coupon

- Basic coupon geometry [5] is 150 mm x 30 mm x 3 mm with Φ10 central hole.
- The designated grip area is 25-35 mm from each longitudinal end.
- The hole has a 45 degree chamfer that is 0.3 mm at base and height.
- Variation to above dimensions is allowed within specification limitations, without implying likeness of result between variations for equivalent loading.
- The specimen is generally clamped by pressure at the clamping area.
- It has a nominal Kt=2.3 (rounded) = Theoretical Gross Ktg / KtG/N
  where, Gross to Nett Section area = KtG/N=1.5, Ktg=3.4 is calculated from [2].

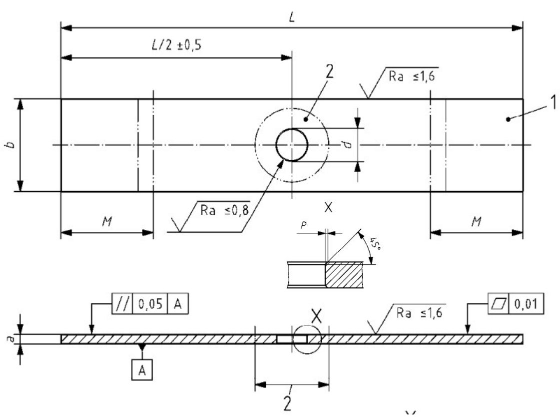

Specimen	*L*	*b*	∅	*M*
T-type	150	30	10	25-35

Thickness *a* [1]	Tolerance ∅ bore		Depth *P*	Concentricity between bore and chamfer
	Others materials [2]	Aluminium alloys		
$3\ ^{0}_{-0,05}$	∅ ± 0,1	$∅\ ^{0}_{-0,04}$	0,30 ± 0,05	≤ 0,03

1 Marking area
2 Calibrated section
M: area for clamping

a =	radius =	5	mm
c =	near edge =	15	mm
e =	far edge =	15	mm

C1 =	3.001
C2 =	0.110
C3 =	1.929
C4 =	6.115
Ktg =	3.479

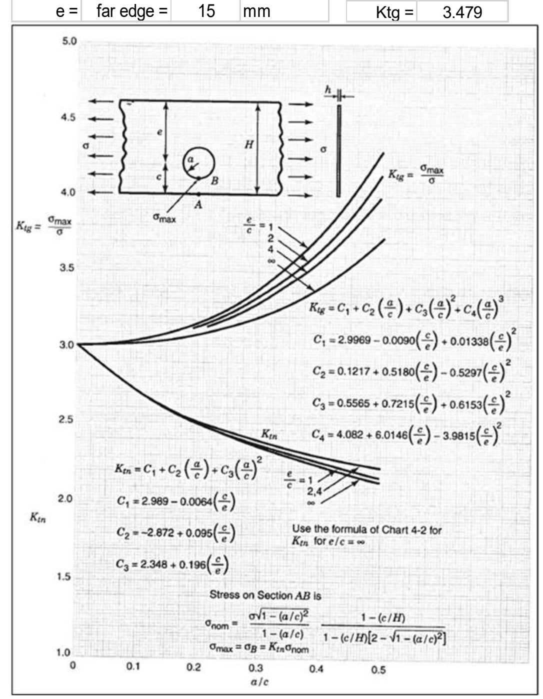

AIRBUS

Concept – geometric modifications initially considered

- Considering space cryogenic applications, cylindrical tanks and pipes are candidates for aircraft application.
- In the interest of mass and manufacturing efficiency – alloy sheets are potential raw material to be tested.
- Mechanical clamping of the coupon need thus be adaptable to specimen that are globally of specimen section *i.e. "thin"*.

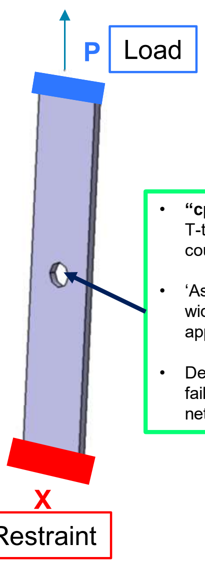

- **"cp0"** – Basic T-type coupon.
- 'As is' and widely applied.
- Designed for failure at the nett section

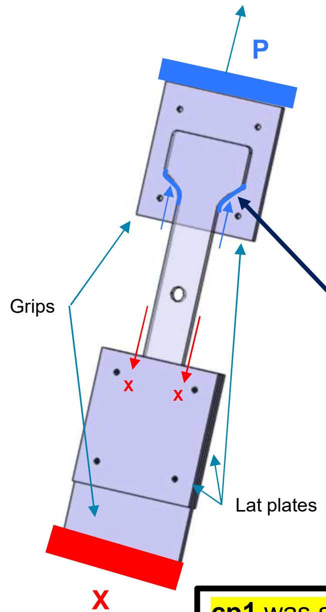

- **"cp1"** – Uniform thickness 'shoulder' specimen (3 mm) loaded mechanically at profiles growing the width at the designated clamping region ("M" [5]) by grips of a stronger and stiffer material.
- The grips in-turn are directly loaded by the frame of testing machine.
- Specimen length is increased by 60 mm while respecting the start of "M".
- Assembly is bolt-clamped laterally using 4 "Lat Plates".
- Minimum hole edge distance = 2 x dia.

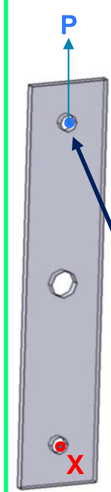

- **"cp3"** – Uniform thickness pin-loaded specimen (3 mm) at the designated clamping region ("M" [5]).
- Pin-holes must be of a lower Ktg than the hole at the test-section although fille.
- Be of transition or low interference fit, to reduce the chance of initiation at loading location.
- No increase in specimen length.

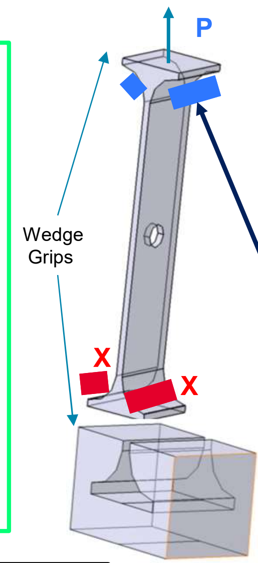

- **"cp4"** – Wedge - loaded specimen modified in thickness with a 'heavy fillet' profile at the designated clamping region ("M" [5]).
- Specimen will be slotted into fixed wedge grips that may be directly linked to
- Be transition or low interference fitted, to reduce chance of initiation at loading location.
- No increase in specimen length.

cp1 was studied, as it is of uniform thickness & with One hole.

Airbus AMBER

Concept – cp1 section determination (initial sizing)

- Assume a force value that approaches failure at the nett section. Half of this is to be borne by each shoulder at an end of a **cp1** specimen.
- Calculate axial stress at the shoulder as σs = Force / (width of load transfer surface 's' x thickness), compare with UTS, to obtain minimum width 'L'
- Assume growing a section at the end of **cp1** in length and width, Calculate Shear Stress from root shear force, compare with Fsu to obtain minimum 'h'.
- Assume growing a section at the end of **cp1** in length and width with Uniformly Distributed Load on this 'cantilever beam', refine L with sufficient reserve (RF).
- A parabolic profile was arbitrarily drawn over the cantilever retaining a 'safe' minimum h=30 mm, fillets applied to ends to smoothen load transfer.

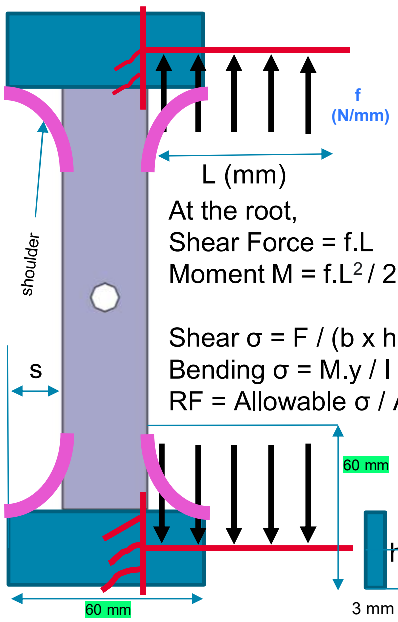

At the root,
Shear Force = f.L
Moment M = $f.L^2 / 2$

Shear σ = F / (b x h)
Bending σ = M.y / I
RF = Allowable σ / Applied σ

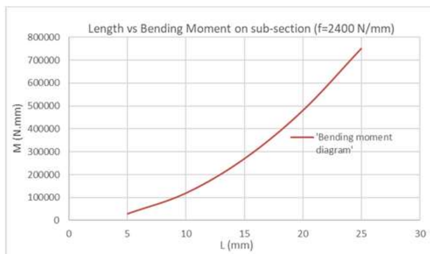

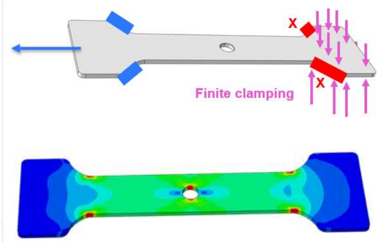

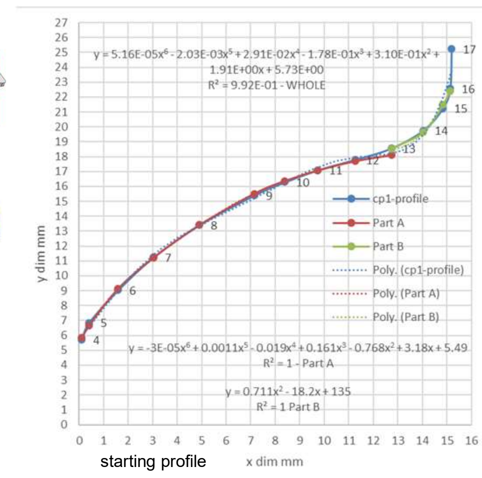

- When loading is idealized using FEM as a standalone part, stress peaking can be seen at fillets of shoulder ends.
- The nett-section still has the highest stress and will fail in uniaxial tension under monotonic loading.
- Failure is not obvious at the shear section or due to bending.
- For simplicity, the Grip and Lat plates will the have same thickness as cp1 (3 mm).

AIRBUS

Airbus AMBER

3. Influence of elastic modulus

AIRBUS

Airbus AMBER

About study of the elastic modulus

- **The stress-strain response of a shape of a given material is indicative of its stiffness with respect to the load path for a manner and magnitude of load. Elastic region response prior to the onset of plasticity is studied**
- **The modelling of pre-failure plasticity can provide a view of the overall response to elasticity.**
- **Stress-strain response is extracted at key "gauge" locations.**
- **It may be a criterion for selection or validation of geometry or materials for a structural concept.**
- **Load applied to model is derived from theoretical coupon material limits to avoid excessive load to FEM**
- **3 Grips x 2 specimen = 6 models. The clamp (AISI 316) is constant.**
- **Peaking location at tie constraints are also considered here as points of interest**
- **Here, load will start transfer between materials of varied stiffness at the start of the tie.**

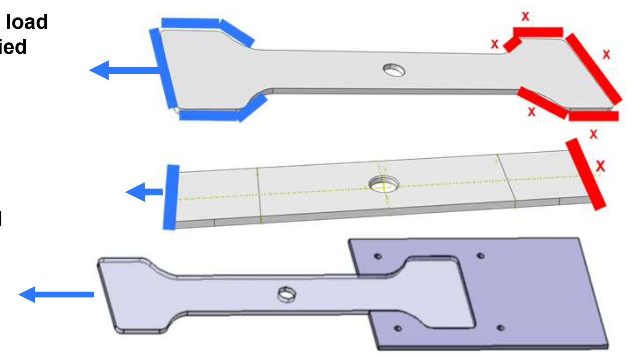

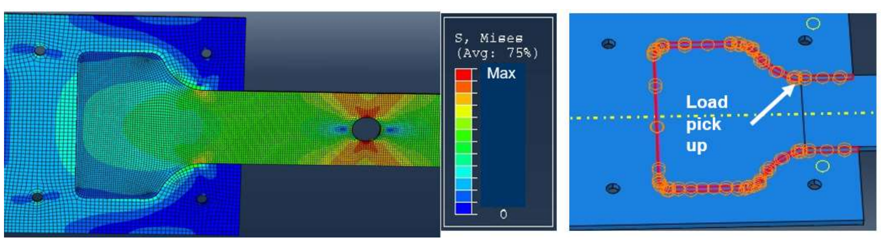

Surfaces assumed to be in contact when loaded, are tied together *from the shoulder radius of the coupon*

For both models compared:
- Hex elements are used.
- **cp1** is tied to grips at the interfacial surface
- One end is encastered.
- The other is point loaded by force and is kinematically coupled at the upper and lower surfaces of the clamp.
- 2 elements across the Grip thickness (1.5 mm size)

For **cp1**:
- **cp1** is tied to grips at the interfacial surface
- Fastening and Lat plates are not modelled here

AIRBUS

Airbus AMBER

Response to material input at the Test Section

- ➔ RO curves vs "mod" curves - exhibits change to plastic shape until UTS.
- ➔ Overall in the linear region – all curves overlap and are in good agreement
- ➔ At the nett section D, cp1 strains more than cp0 & sees higher stress.
- ➔ Whereas at B, cp1 also sees the same compared with cp0. Comparing B12 with B132 higher plasticity hence earlier failure of cp1 is anticipated compared to cp0. Conservative?
- ➔ Test section peak C shows a greater stress at C1x2 & C4x2, thus cp0 failure may precede cp1.
- ➔ The gross section A shows a general uniformity between configurations and does not see the onset of yield while the test section sees UTS.
- ➔ Lateral deflection tendency of the grip may be reduced by bolting of Lat plates.

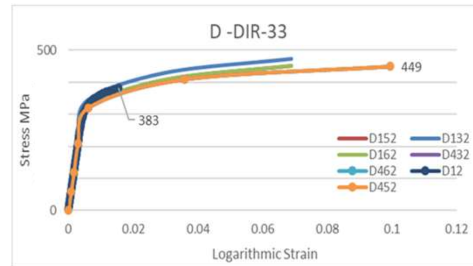

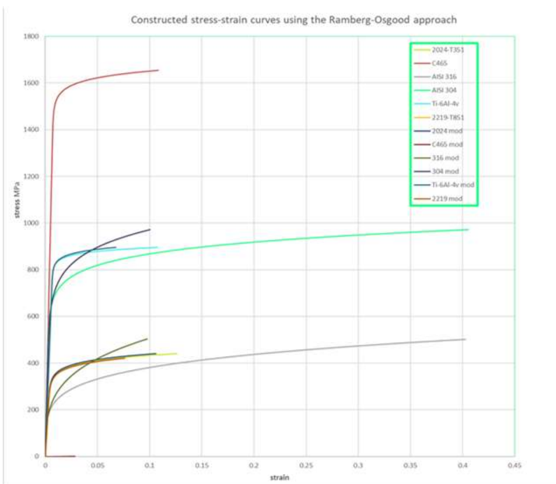

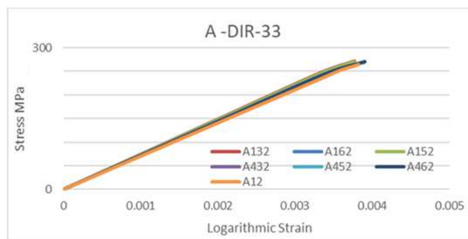

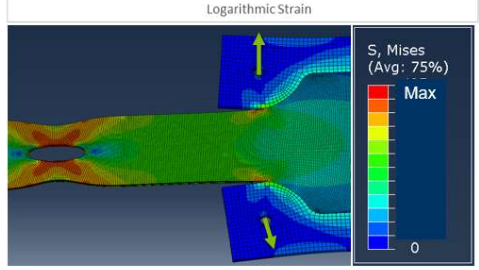

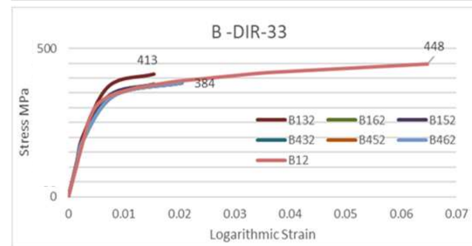

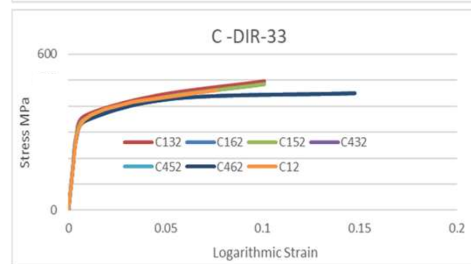

AIRBUS

Response to material input at the Grip and Shoulder

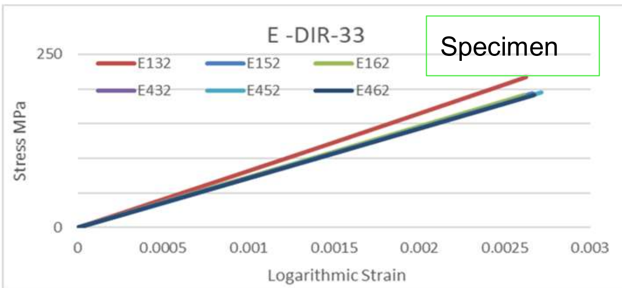

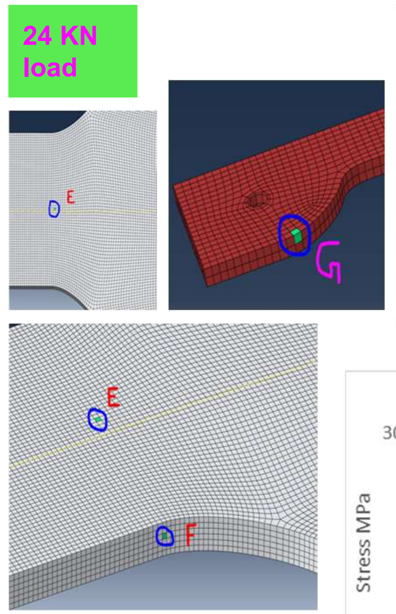

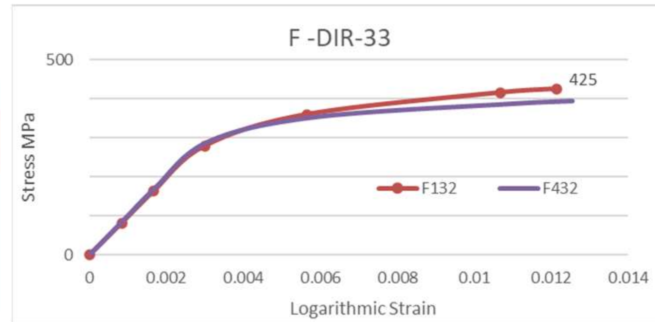

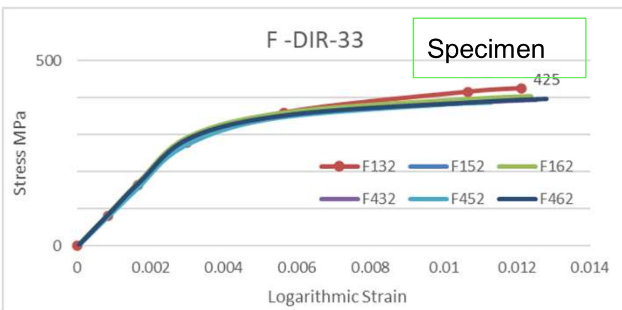

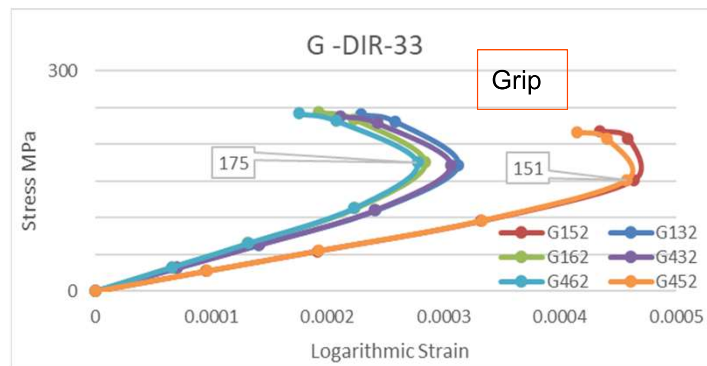

- ➔ At shoulder field E, only by E132 is a marginally higher stress seen.
- ➔ A similar observation at the shoulder F132, although the magnitude is high.
- ➔ The gap between 132 & 432 may be attributed to the assumed failure strains.
- ➔ At the grip peak G, a local strain relief with increasing stress is seen as the assembly adjusts to displacement.

5. Assembly clearance and friction

Airbus AMBER

Approaches to modelling of 0.4 mm assembly gap - observations by constraint

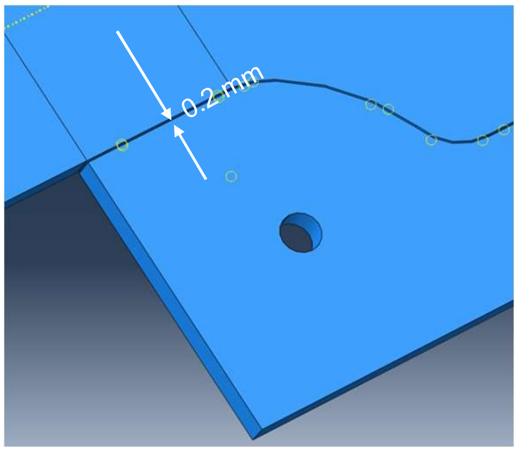

- Surface contact within 'General contacts' was used to model 0.2 mm edge clearance.
- Transition in distribution reflects lateral deflection of the grip, holding the peak stress.
- At cp1, the peak observed with modelling of the gap now lies at the tip of the shoulder.
- A μ value was required to constrain the model but the appropriate value between Al. and Steel lies between 0.2 and 0.8 [10][11].

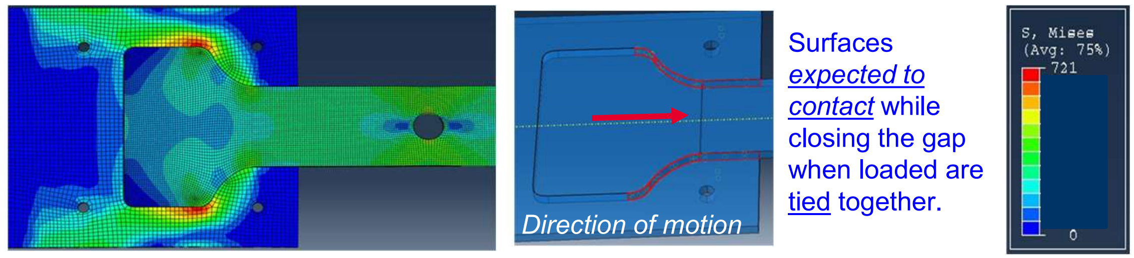

Surfaces *expected to contact* while closing the gap when loaded are tied together.

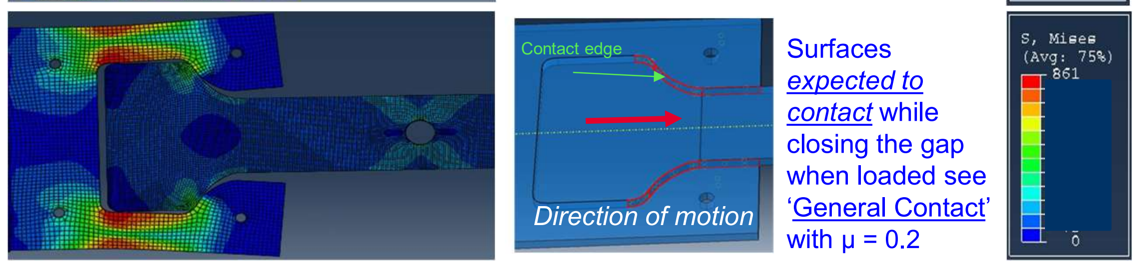

Surfaces *expected to contact* while closing the gap when loaded see 'General Contact' with μ = 0.2

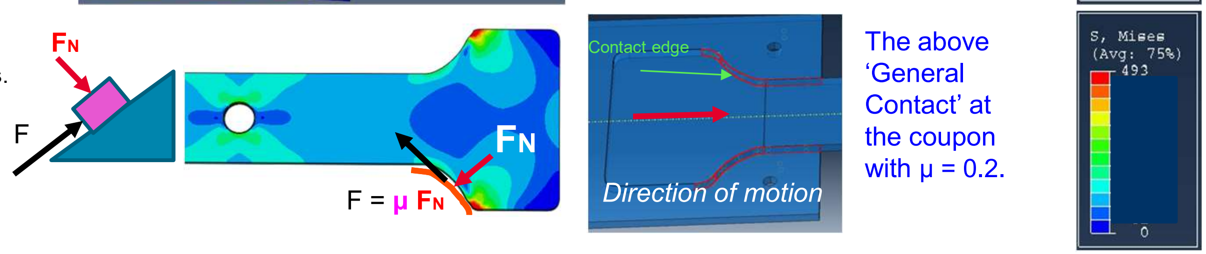

The above 'General Contact' at the coupon with μ = 0.2.

- **With 0.4mm clearance, grip stress distribution shifts towards the base of the specimen as it bends. This now has the peak value.**

The effect of static friction on simulated displacement

- It was experimentally shown within Ref. [10] that static friction μ varied with applied stress but tends to a non-linear stabilization path after 50 MPa.
- The specimen which was displacement loaded would plateau at a value of force, for μ = 0.6, which was selected due to location at the end of the 'linear' portion of the curve (Fig. 5, Ref. [10]).
- The reacted force however was seen to somewhat increase with μ while the stress distribution at the grip was variable until a finite value. Beyond this, it redistributes into the coupon as can be seen below for μ = 1.8. *Although peak stress reduces with μ, area distribution of high stresses increases at the grip.*
- Friction provides increasing restraint to **cp1** with respect to the grip. Modelling of bolting is expected reduce lateral deflection to realistic assembly magnitude.

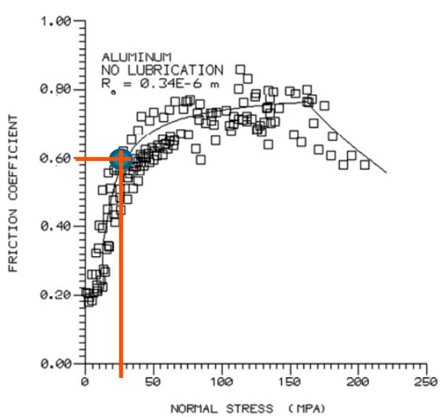

Fig. 5, Ref. [10]

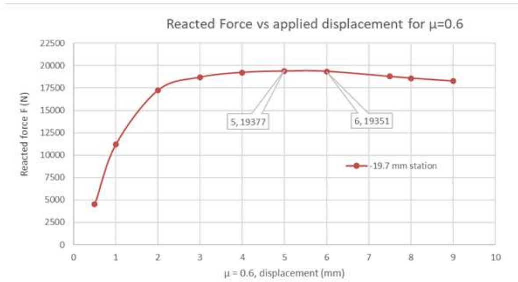

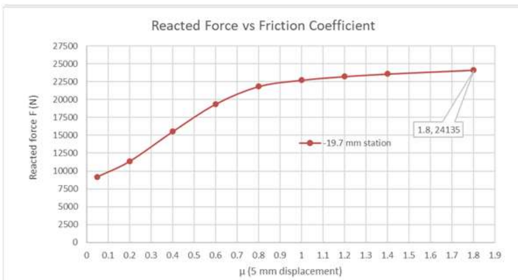

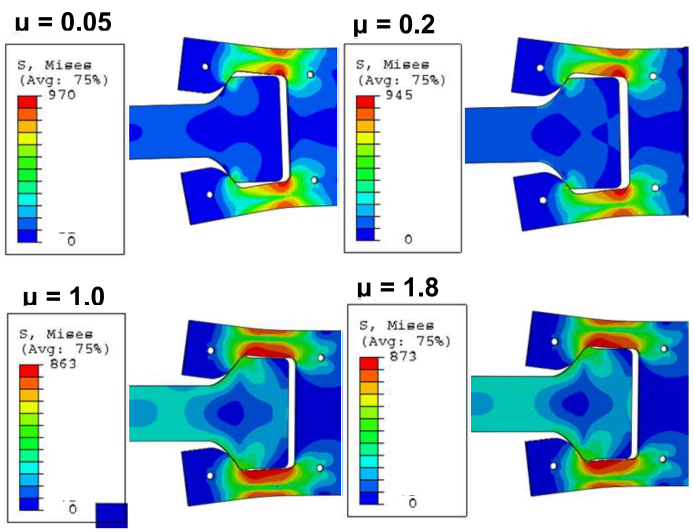

6. Bolting and clamping

Modelling of bolting arrangement

Bolts are stiff and strong members which serve both as beams and springs that are used to connect structures. They generally are primarily loaded in shear and additionally pre-loaded by torquing, to be in tension.

- At first, the mechanical stiffness is modelled – it is a function of E of the plates and bolt, plate thicknesses and bolt shank diameter. The stiffness of a bolt determines the amount of load transferred to connecting plates.
- When sizing, it would be conservative to have stiffness values higher than those expected from the connection.
- 3 mm Lat plates were modelled with mesh density identical to the grip i.e. with 2 elements through the thickness.
- 1D Fasteners were constructed by linking end-nodes of CONN3D2 elements between successive plates by use of *continuum distributing couplings* which couple motion of the reference node to the average translation of the coupling nodes and distribute the forces and moments at the reference node as forces only.
- Arbitrary stiffness values of K = 1,000,000 N/mm was specified for all directions.
- The model was run and connector forces extracted to use for shear sizing of bolts.

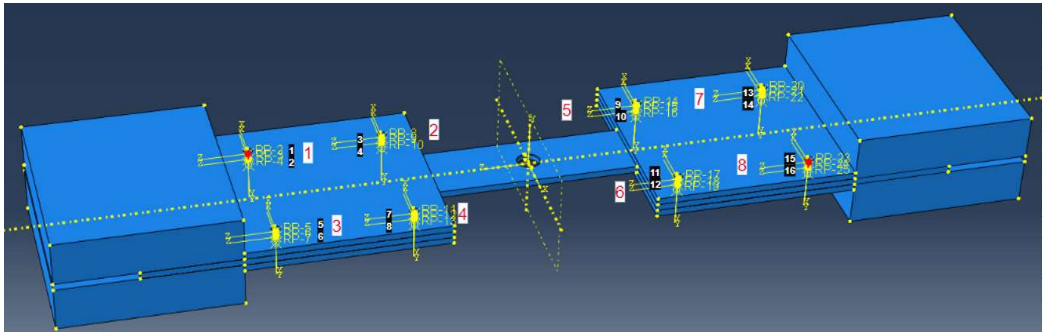

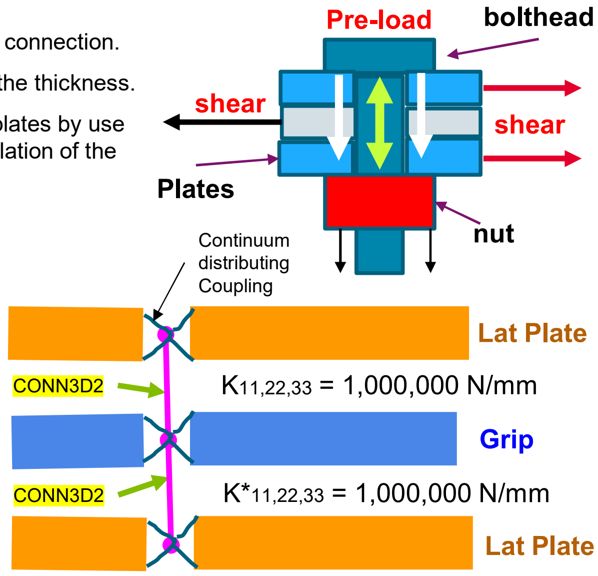

*D_{11}, D_{22}, D_{33} in Abaqus

Airbus AMBER

Bolt loads in shear

- Forces extracted are the result of plates withstanding both the longitudinal pull and lateral deflection. The latter is the worst case.
- Shown below is the forces profile as the joint is loaded to failure strain. The maximum force 4240 N is small compared to double-shear allowables from EN 6115 [12].

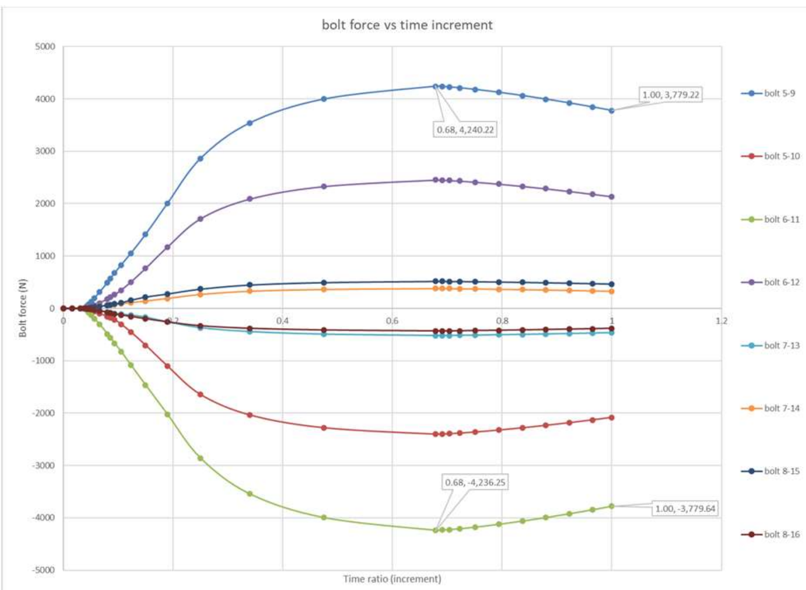

Dia. code No.	Min. double shear strength (N)		
	Steel alloy	Titanium alloy	Ni-based alloy
2	–	17 760	–
3	27 250	23 900	31 500
3A	–	32 000	41 600
4	47 150	41 330	54 800
5	73 850	64 880	85 100
6	106 300	93 320	123 000

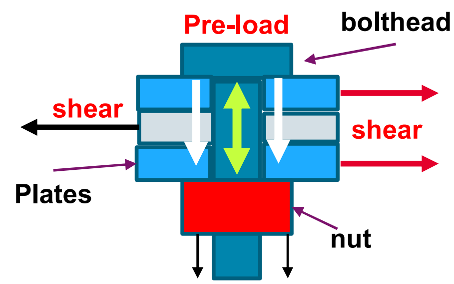

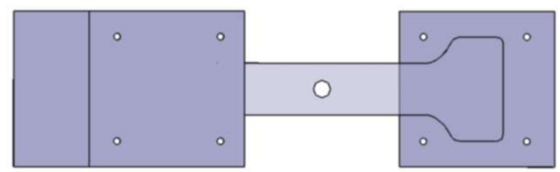

AIRBUS

The effect of 1-D bolting upon the FEM

- A significant redistribution of stress is seen as a result of fastening as lateral displacement of the grip is curbed by bolting.

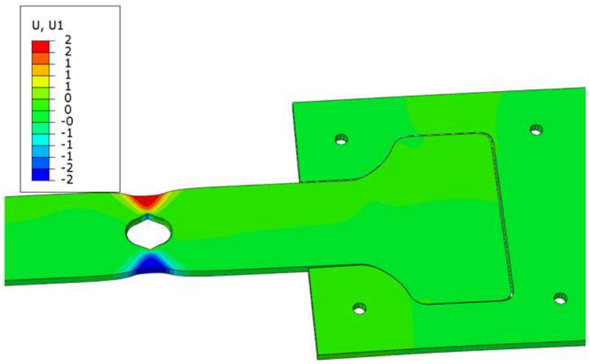

- The stress at the grip although well below its TYS at specimen failure load, it is higher than the Fsu (530 MPa). Fatigue test would however operate at a significantly lower stress level, lying below cp1's TYS.
- Failure of the specimen certainly occurs at the Nett section.
- While the specimen does enter yield at the shoulder (346.9 MPa), this is 29.8 % lower than the nett-section at 494 MPa.

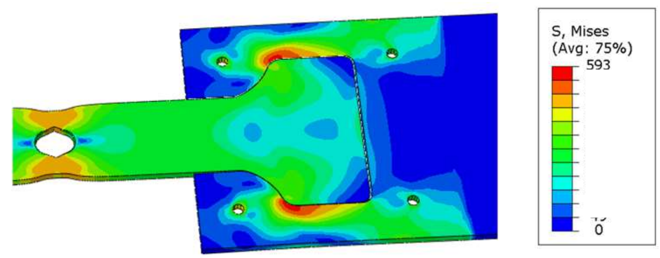

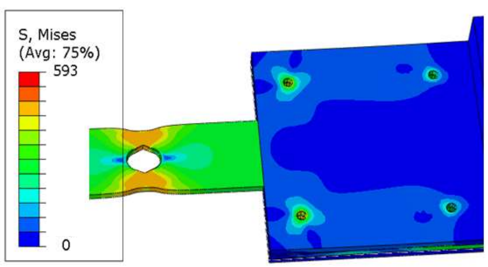

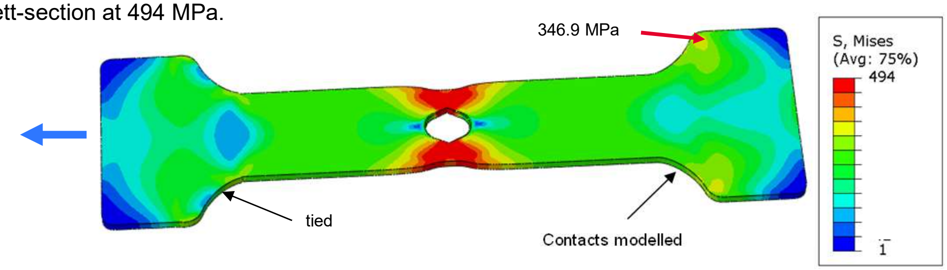

AIRBUS

The effect of clamping

Clamping will result in reduction of z-stress and redistribution outside the clamped region.

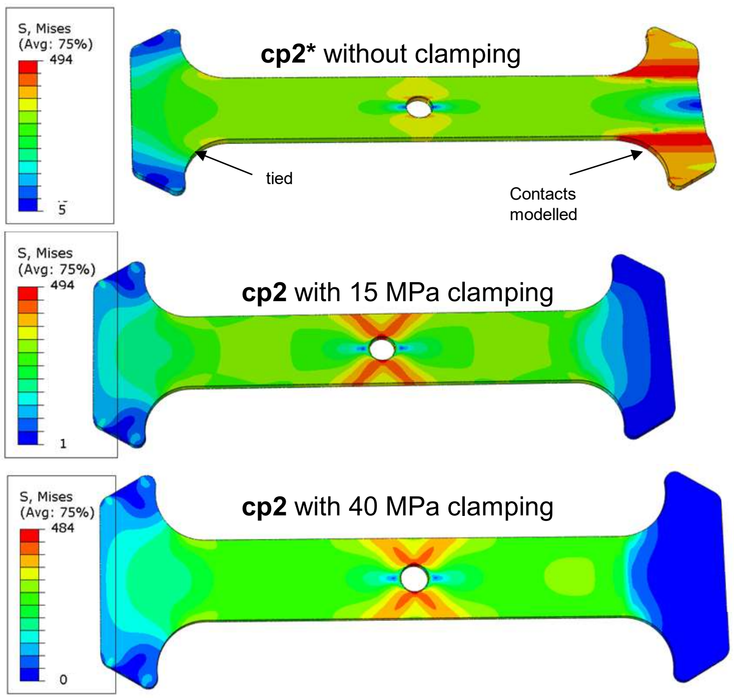

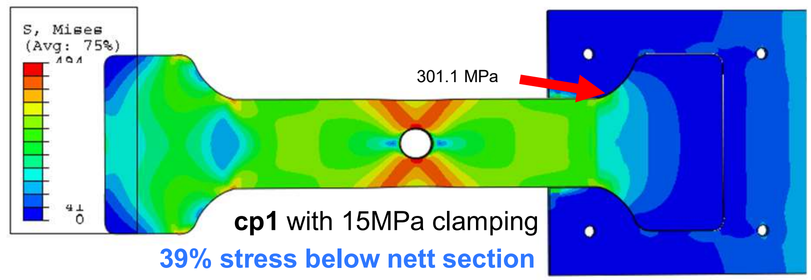

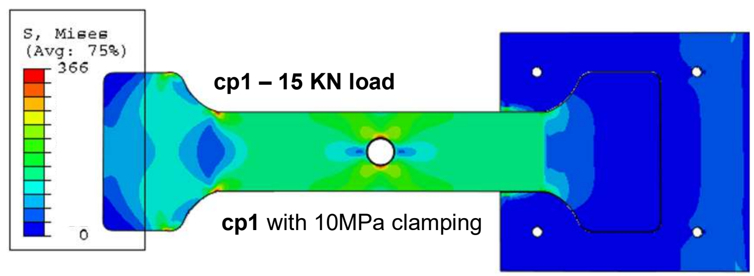

- **Loaded in the vicinity of yield, initiation is predicted to occur at the nett-section. This is conservative for fatigue testing.**

***cp2** is a **cp1** variant with long moment arms and low ‘h’ at the shoulder.

Airbus AMBER

Bolt sizing

- Clearly the bolt will be sized by the clamping force of 10 MPa.
- Total clamping force = Clamping Pressure x Area of clamping surface
- Force per fastener is dependent upon the layout. In this case it will be evenly divided.

Clamping pressure =	10	MPa
Lat Plate dimension L =	90	mm
Lat Plate dimension B =	90	mm
dia. of hole =	6.35	mm
Area of hole =	31.7	mm2
No. of holes =	4.0	
Surface area calc. =	7973.3	mm2
Clamping force =	79733.2	N
Force / fastener =	19933	N

Min. tensile strength (N)		
Steel alloy	Titanium alloy	Ni-based alloy
–	9 660	–
17 100	14 150	20 820
–	17 800	25 060
29 150	25 900	35 490
46 050	40 900	56 070
70 050	62 250	85 300

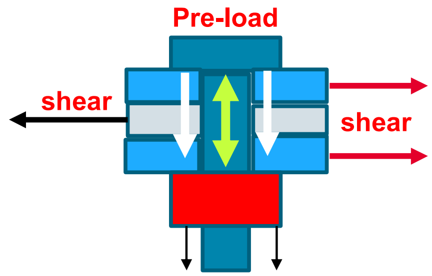

Let us choose the EN6115K Titanium fastener – Size 4

- The force is lower than the tensile allowable of a shank for a Size 4 bolt (nominal Φ = 6.35mm)
- The selected nut is to internal specification ABS 1826, based upon fastener size.

Bolt Tensile strength =	25900	N [12]
Nut Tensile strength =	23500	N

Corresponding Torque	Dia Code V	min V	nom V	max V	
	4	7.6	8.6	9.8	N.m

Sized by nut tensile strength, RF = 1.17 when the assembly is loaded to failure

- As general practice, nominal torque corresponds to 0.7 x Bolt UTS = 18130 N
- Since this is lower than the clamping force, a torque value between nominal and maximum is suggested.
- To reduce this force, the joint may use more fasteners (ex. 6).
- Huth Stiffness [8] was calculated. K11,33 = 59484 N/mm, K22 = 615016 N/mm, which is lower than our assumption of 10E6 N/mm.
- Gray & McCarthy's approach [9] is an alternative said to 'relieve' the shear stress values predicted by Huth.

7. Energy consideration

Airbus AMBER

Need and Approach to failure energy estimation

- The energy during failure (by fracture) can serve as a direct basis of comparison in design towards structural equivalence. Abaqus damage modelling is applied to different coupon geometries applying internally calibrated material data for 2024-T351. Explicit linear elements were assigned to the coupon with global size 0.75 mm.
- Study on energy absorption behaviour of a material requires a careful consideration of a coupon design, the assignment of calibrated material model and capturing relevant mechanical responses. In our work calibrated AA2024 was assigned to the coupon which offers both Elasto-plastic material response and damage response.
- Explicit Dynamic modelling was used to simulate the tensile testing. Response time of 0.02 sec enabled efficient computing while keeping the kinetic energy to the minimum range compared to Internal Energy.
- Assigning smooth amplitude ensures that the applied load is transferred to the coupon without sudden movements which can cause stress waves and induce noisy or inaccurate solutions.
- In the field output, Damage initiation criteria was invoked to ensure that elements are appropriately removed in the region of stress concentration.
- In the history output, force and displacement curves were captured with sufficient points via anti-aliasing filter option.
- Coupons are modelled as standalone with representative constraints.

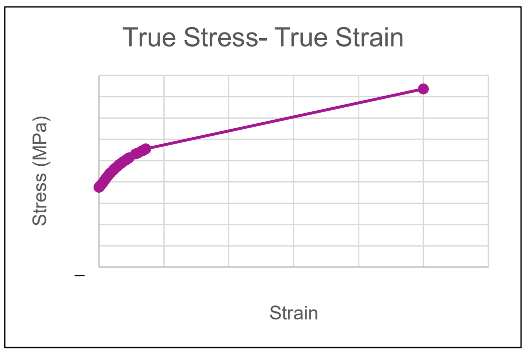

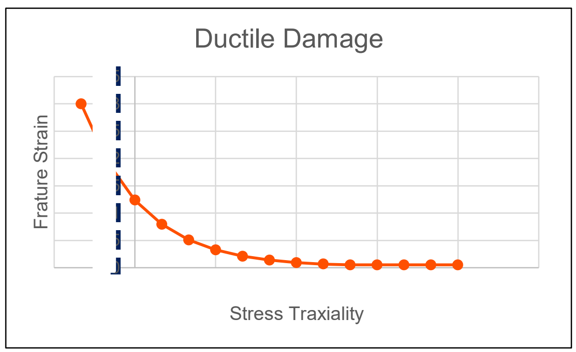

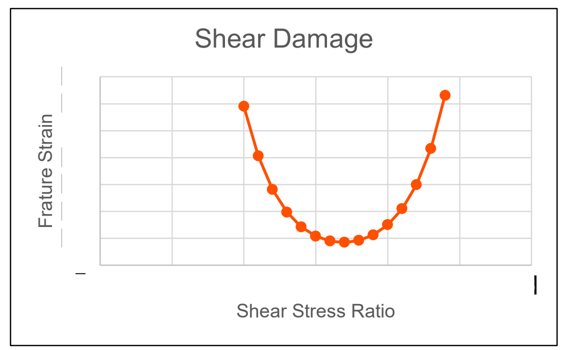

AIRBUS

Energy estimation

A Force-displacement curve of the loading point was extracted as a history output from Abaqus. Its equation is integrated within limits of extracted data to calculate the area under the curve, which is the energy absorbed in Joules. While **cp1** has a fracture energy that is nearest to **cp0**, **cp4** would be the most conservative specimen.

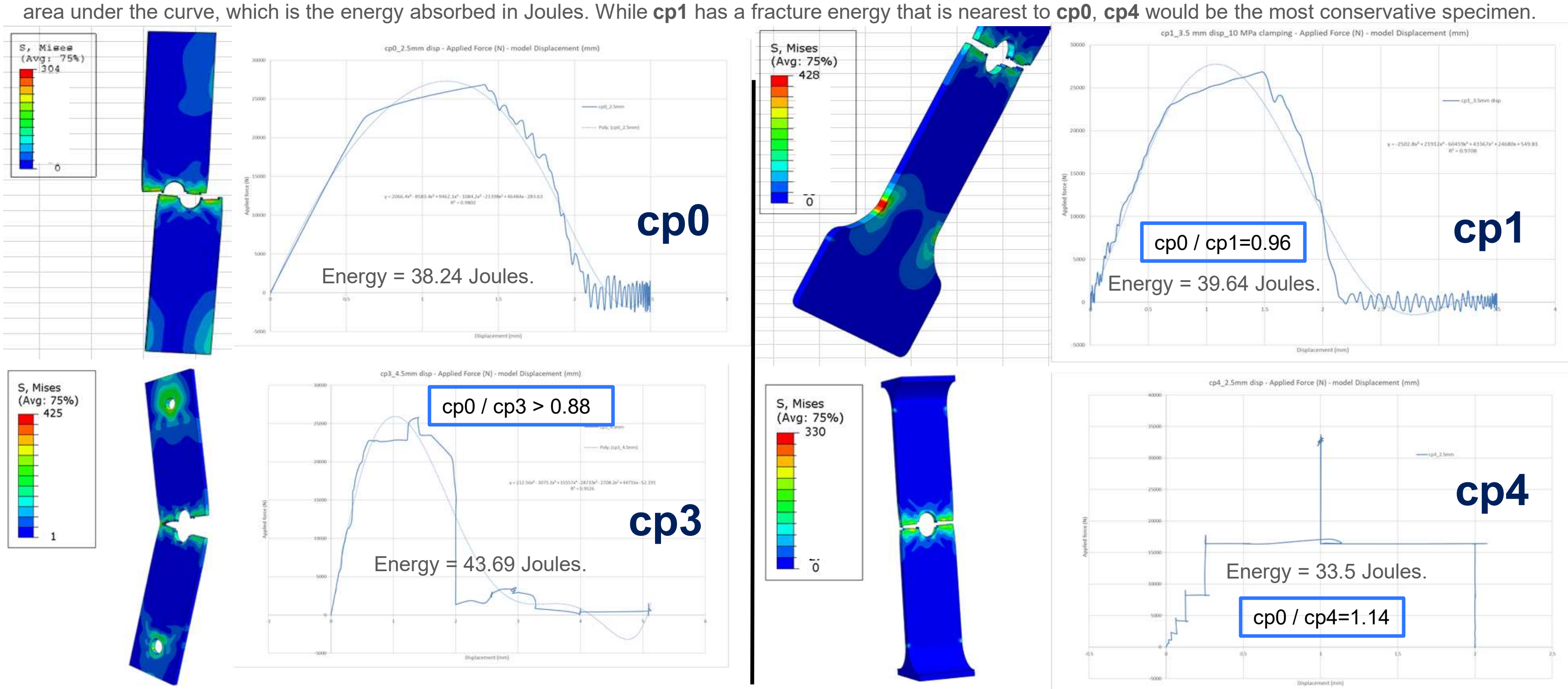

8. Summary

To summarize

- From comparison of damage to **cp0** with **cp1**, the ratio of energy absorbed = 38.24 / 39.64 = 0.96.
  Appropriately constrained, they are expected to perform similarly in test.
  Initial sizing of the coupon shoulder is based upon:
  1) Shoulder axial stress
  2) Shear force at the root
  3) Parabolic curve of the bending moment diagram

- Grips are sized and theoretically assessed to be suitable for application with the proposed geometry of **cp1** specimen.
  While most of the operation of grips is expected to be within the material's endurance limit, it is expected that cycles of service performed at higher stress levels be recorded in order to be able to estimate its remaining life using the cumulative damage approach.

- Appropriate clamping enables reduction of stress at the shoulder and re-distribution to the nett-section. Appropriate clamping can mitigate drawbacks of the shoulder profile.

- Further work:
  - Sizing study by considering thermal expansion is due for the design phase associated with characterization at cryogenic temperature.
  - The experimental correlation of present work is to be completed.

Thank you

AIRBUS